

# Population labeling spectroscopy for the electronic and the vibrational transitions of 2-pyridone and its hydrogen-bonded clusters

著者	三上 直彦
journal or publication title	Journal of chemical physics
volume	113
number	2
page range	573-580
year	2000
URL	<a href="http://hdl.handle.net/10097/35713">http://hdl.handle.net/10097/35713</a>

doi: 10.1063/1.481833

# Population labeling spectroscopy for the electronic and the vibrational transitions of 2-pyridone and its hydrogen-bonded clusters

Yoshiyuki Matsuda, Takayuki Ebata,<sup>a),b)</sup> and Naohiko Mikami<sup>a)</sup>

Department of Chemistry, Graduate School of Science, Tohoku University, Sendai 980-8578, Japan

(Received 25 January 2000; accepted 10 April 2000)

The  $S_1$ – $S_0$  electronic spectra, and the vibrational spectra of jet-cooled 2-pyridone (2PY) and its hydrogen bonded clusters, 2PY–H<sub>2</sub>O and 2PY dimer, have been investigated by population labeling and various double-resonant vibrational spectroscopies. For bare 2PY, the  $S_1$ – $S_0$  spectrum was measured by laser-induced fluorescence and population labeling spectroscopy. In addition, IR and Raman spectra of the NH stretching vibration were observed in  $S_0$  and  $S_1$ . The results led to the conclusion that 2PY has two close lying electronic states in the  $S_1$  region, whose structures are slightly different with respect to the NH group. It was also found that the NH stretching frequency becomes smaller in  $S_1$  than in  $S_0$ , indicating that the NH bond strength of 2PY becomes weaker in  $S_1$ . The effect of the electronic excitation on the hydrogen bond strength has also been investigated by measuring the NH and OH stretching vibrations of the hydrogen bonded clusters in the two electronic states, and it was found that the hydrogen-bond strength is weaker in  $S_1$  than in  $S_0$ . For 2PY dimer, the IR and the Raman spectra of the NH stretching bands showed a clear intensity alternation, confirming its  $C_{2h}$  symmetric structure. © 2000 American Institute of Physics. [S0021-9606(00)00626-7]

## I. INTRODUCTION

2-pyridone (2PY) is a simple molecule having a peptide group and it exhibits two stable tautomeric forms, 2PY and 2-hydroxypyridine (2HP), as shown in Fig. 1(a). Many spectroscopic and theoretical studies have been done on the keto-enol tautomerization of 2PY.<sup>1–37</sup> In the gas phase,<sup>4,6,8,11,12,20</sup> the 2HP form is thought to be  $\sim 200$  cm<sup>–1</sup> more stable than the 2PY form, and the tautomerization barrier is estimated to be 20 000 cm<sup>–1</sup>.<sup>23</sup> For 2PY in a protic solvent, it is expected that the barrier is substantially reduced by forming hydrogen bond with solvent molecules. In such a solution, the tautomerization reaction proceeds through the exchange reaction of protons between 2PY and solvent molecules. In this respect, spectroscopic studies on the structure of its hydrogen-bonded clusters are of special importance for the understanding of the keto-enol tautomerization in the molecular level.

The electronic spectra of 2PY and its clusters have been studied in supersonic jets by several workers.<sup>38–44</sup> In particular, Bernstein's group<sup>38</sup> performed detailed analyses of the  $S_1$ – $S_0$  electronic transition of jet-cooled 2PY and its hydrogen bonded clusters by measuring the fluorescence spectra and mass-resolved resonance enhanced multiphoton ionization spectra. Later, Pratt's group observed rotationally resolved laser-induced fluorescence (LIF) spectra of 2PY, 2PY–H<sub>2</sub>O, and (2PY)<sub>2</sub>, and determined their structures.<sup>39–43</sup> These studies gave us the detailed information for the electronic spectra and their structures. However, until very recently, there has been no spectroscopic study on the NH or OH stretching vibration in supersonic jets. These

vibrations may provide us with the direct information on the keto-enol tautomerization and on the hydrogen-bonding structure of the clusters. Actually, many of the studies in bulk phase reported the vibrational spectra of these modes.<sup>4,6,8,28,32,37</sup> In our previous paper, we first reported the measurements of the vibrational spectra of the NH and CO stretching vibrations of 2PY and the OH stretching vibration of its clusters.<sup>45</sup> By comparing the observed spectra with the simulated ones of the energy optimized structures obtained by *ab initio* molecular orbital calculations, we succeeded in characterizing the vibrations and the cluster structure.

In the present work, we have mainly investigated the structures of 2PY and its clusters in the  $S_1$  state. There are several interesting problems of 2PY in  $S_1$ . First is the presence of two intense bands (we call bands A and B) in the  $S_1$  electronic region of 2PY. The two bands were first suggested to the transitions of two isomers of 2PY by Nimlos, Kelley, and Bernstein.<sup>38</sup> Later, Held, Champagne, and Pratt<sup>39</sup> measured high resolution electronic spectra of the two bands, and concluded that the two bands are the transitions from the same zero-point level but to the different upper states having different structures. In our previous paper, we supported the conclusion of Held and co-workers since the IR–UV double resonance spectra associated with the two bands exhibit the same frequency for the NH stretching vibrations in  $S_0$ .<sup>45</sup> In the present work, we measured the population labeling spectra for the two bands. In addition, we obtained more precise NH stretching vibrational frequency by measuring the Raman spectra. These results provided us with firm evidence that the two bands originate from the same zero-point vibrational level. In addition, we investigated the fluorescence quantum yield of 2PY by comparing the LIF and the popu-

<sup>a)</sup>Authors to whom correspondence should be addressed.

<sup>b)</sup>Electronic mail: ebata@qclhp.chem.tohoku.ac.jp

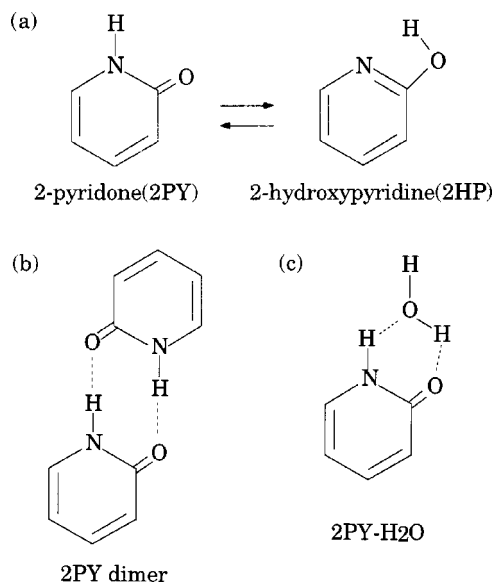


FIG. 1. Schematic representation of the stable structure of (a) 2PY and 2HP tautomers, (b) (2PY)<sub>2</sub>, and (c) 2PY-H<sub>2</sub>O.

lation labeling spectra and found that the yield rapidly decreases with the excitation energy.

Second is the effect of the electronic excitation on the tautomerization reaction of 2PY in the isolated condition and also in the hydrogen-bonded clusters. Though the barrier height for the tautomerization reaction is very large in  $S_0$  ( $\sim 20\,000\text{ cm}^{-1}$ ), it is expected that the large exothermicity ( $6500\text{ cm}^{-1}$ ) from 2HP to 2PY may decrease the barrier height in  $S_1$ .<sup>38</sup> In addition, the electronic excitation also changes the ability of the hydrogen bonding of 2PY. Such changes may drastically affect the potential energy surface, especially along the coordinates of the NH and OH stretch modes, leading to substantial changes in their vibrational energies. So, we measured the NH vibration of 2PY and also the OH stretching vibration of its clusters in  $S_1$  to find an indication of the tautomerization.

Finally, we investigated the structure of (2PY)<sub>2</sub> by measuring the IR and the Raman spectra of its NH stretching vibration. From theoretical works<sup>28,44</sup> and an analysis of the high-resolution electronic spectrum,<sup>43</sup> (2PY)<sub>2</sub> is thought to have a planar  $C_{2h}$ -symmetric structure and a large binding energy. Such a large binding energy and the high symmetry structure of (2PY)<sub>2</sub> can also be confirmed by observing the NH stretching vibration and its IR and Raman activities.

## II. EXPERIMENT

Supersonic jets of 2PY and its clusters were generated by expanding a gaseous mixture of 2PY and solvent molecules, seeded in 3 atm of He carrier gas, into vacuum through a pulsed nozzle having a 0.8 mm orifice. To obtain sufficient vapor pressure, a sample compartment of 2PY crystal was heated at 370 K. We applied various double resonant spectroscopic techniques for jet-cooled 2PY and its clusters as shown in Fig. 2. For the electronic spectrum measurement, we used population-labeling spectroscopy, as shown in Fig. 2(a). For the vibrational spectroscopy of the

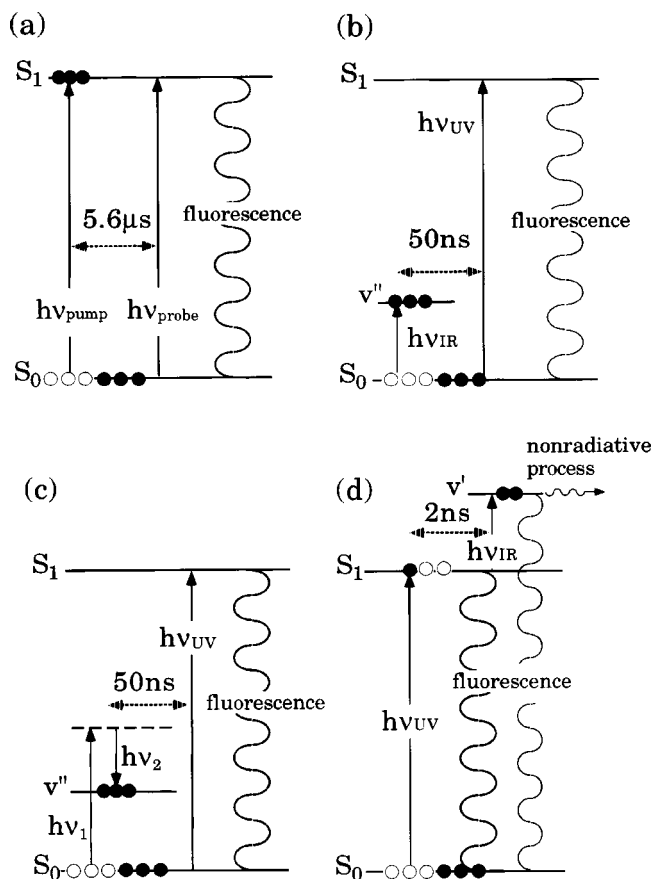


FIG. 2. Excitation schemes of (a) population labeling, (b) IR-UV double-resonance, (c) stimulated Raman-UV double-resonance, and (d) UV-IR double-resonance spectroscopy.

NH and OH stretching vibrations in  $S_0$ , we used IR-UV double-resonance [Fig. 2(b)] and stimulated Raman-UV double-resonance spectroscopies [Fig. 2(c)] with fluorescence detection. For the observation of the vibrations in  $S_1$ , we applied UV-IR double-resonance spectroscopy with fluorescence detection, as shown in Fig. 2(d).

### A. Population labeling spectroscopy

The experimental setup for population labeling spectroscopy was described in detail elsewhere.<sup>46</sup> In this spectroscopy, the frequency of the probe laser ( $\nu_{\text{probe}}$ ) was fixed to the  $S_1$ - $S_0$  transition of a specific species in the supersonic free jet and its ground state population was monitored by the LIF intensity. Under this condition, a pump laser ( $\nu_{\text{pump}}$ ) was introduced to the jet prior to the  $\nu_{\text{probe}}$  pulse. The power of  $\nu_{\text{pump}}$  was intense enough to deplete the ground state population when its frequency was resonant with the electronic transition. Thus, by scanning  $\nu_{\text{pump}}$  frequency while monitoring the fluorescence intensity, the  $S_1$ - $S_0$  electronic spectrum of the selected species was obtained as a fluorescence-dip spectrum. The two laser beams were introduced into the vacuum chamber and  $\nu_{\text{pump}}$  crossed the jet at 5 mm downstream of the nozzle. The  $\nu_{\text{probe}}$  beam was directed antiparallel to the  $\nu_{\text{pump}}$  beam and crossed the jet at 10 mm downstream of the crossing point of  $\nu_{\text{pump}}$ . The delay time between  $\nu_{\text{pump}}$  and  $\nu_{\text{probe}}$  was set to 5.6  $\mu\text{s}$ .

## B. IR–UV and stimulated Raman–UV double-resonance spectroscopy

The IR–UV and stimulated Raman–UV double-resonance spectroscopies with fluorescence detection were described in detail elsewhere.<sup>47–52</sup> In these spectroscopies, the population depletion induced by a tunable IR laser ( $\nu_{\text{IR}}$ ) or by stimulated Raman pumping was monitored by the  $S_1$ – $S_0$  LIF intensity with a tunable UV laser ( $\nu_{\text{UV}}$ ). We call these spectroscopies fluorescence-detected IR spectroscopy (FDIRS) and fluorescence-detected stimulated Raman spectroscopy (FDSRS). These laser beams were introduced into the vacuum chamber from the opposite direction with each other and were focused onto the jet. The delay time between  $\nu_{\text{IR}}$  or two lasers for Raman pumping and  $\nu_{\text{UV}}$  was fixed to 50 ns.

## C. UV–IR double-resonance spectroscopy

The experimental setup of the UV–IR double-resonance spectroscopy is very similar to the IR–UV double-resonance spectroscopy.<sup>53</sup> In this spectroscopy, the fluorescence intensity was used as a measure of the population in  $S_1$ . Under this condition, the  $\nu_{\text{IR}}$  pulse was introduced at a delay time of 2 ns from the  $\nu_{\text{UV}}$  pulse. The fluorescence quantum yield of the vibronic level of  $S_1$  is usually smaller than that of the zero-point level, so that the total fluorescence intensity decreases when  $\nu_{\text{IR}}$  is resonant with the vibrational transition in  $S_1$ . Thus, the IR spectrum of the  $S_1$  state is also obtained as a fluorescence-dip spectrum by scanning IR frequency while monitoring the LIF intensity.

The tunable IR laser light ( $\nu_{\text{IR}}$ ) for the IR–UV double-resonance spectroscopy was generated by a difference frequency generation between the second harmonic of an injection seeded Nd:YAG laser (Quanta-Ray GCR/230) and an output of the Nd:YAG laser pumped dye laser (Continuum ND 6000), with a LiNbO<sub>3</sub> crystal. For the stimulated Raman pumping spectroscopic measurement, the same Nd:YAG/dye laser system was used. The  $\nu_{\text{UV}}$  source for the probe was a second harmonic of a XeCl excimer laser pumped dye laser (Lambda Physik LPX100/FL3002). The laser beams were focused by  $f=250$  mm lenses. The delay time between the lasers was controlled by a digital pulse generator (SRS DG 535).

The fluorescence of 2PY or its clusters was detected by a photomultiplier tube (Hamamatsu Photonics 1P28) after passing a bandpass filter. The photocurrent was integrated by a boxcar integrator (Par model 4400/4420) connected by a personal computer. 2-pyridone was purchased from Wako Chemical Industries, Ltd. and was used without further purification.

## III. RESULTS AND DISCUSSION

### A. $S_1$ – $S_0$ electronic spectra and Raman spectra of the NH stretch band of 2PY, 2PY–H<sub>2</sub>O, and (2PY)<sub>2</sub>

#### 1. 2PY

The  $S_1$ – $S_0$  LIF spectrum of jet-cooled 2PY in the band origin region is shown in Fig. 3(a). The two intense bands at 29 831 (band A) and 29 928 (band B) cm<sup>−1</sup> were first as-

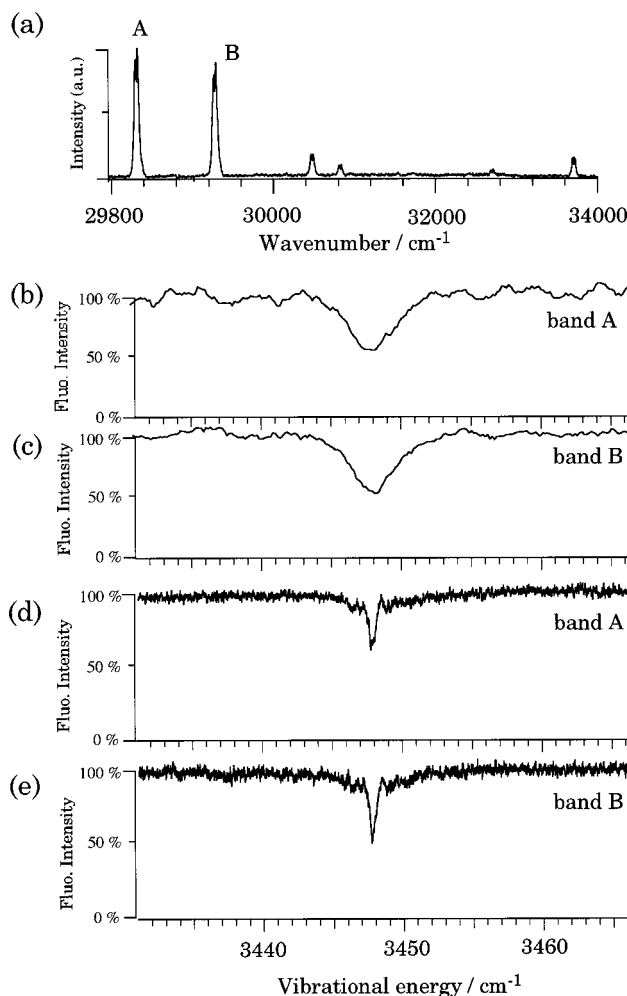


FIG. 3. (a)  $S_1$ – $S_0$  LIF spectrum of 2PY monomer in the band origin region. (b), (c) FDIR spectra obtained by monitoring bands A and B. (d), (e) FDSR spectra obtained by monitoring bands A and B.

signed to the 0–0 bands of different isomers of 2PY in  $S_0$  by Nimlos, Kelley, and Bernstein,<sup>38</sup> while Held, Champagne, and Pratt<sup>39</sup> assigned them to the transitions from the zero-point level of the same isomer to the different excited states having different structures. In our previous paper, we measured the IR spectra of the NH stretching band in  $S_0$  for the two bands, which are reproduced in Figs. 3(b) and 3(c). Since the obtained NH vibrational frequencies were the same for the two bands, we concluded that the bands A and B are originated from the same isomer of  $S_0$ .

In the present work, we first measured the FDSR spectrum of the NH stretch vibration for the bands A and B, to confirm the above-mentioned conclusion. In the Raman spectrum, the  $Q$ -branch intensity is dominant for the totally symmetric vibration, such as the NH stretching vibration, and the band of this vibration in the FDSR spectrum is sharper than that of the FDIR spectrum, providing us with more precise vibrational frequency. Figures 3(d) and 3(e) represent the FDSR spectra for the bands A and B, which are compared with the FDIR spectra [Figs. 3(b) and 3(c)]. The observed NH stretching frequency of 3447.7 cm<sup>−1</sup> in the Raman spectra are the same for the bands A and B, confirm-

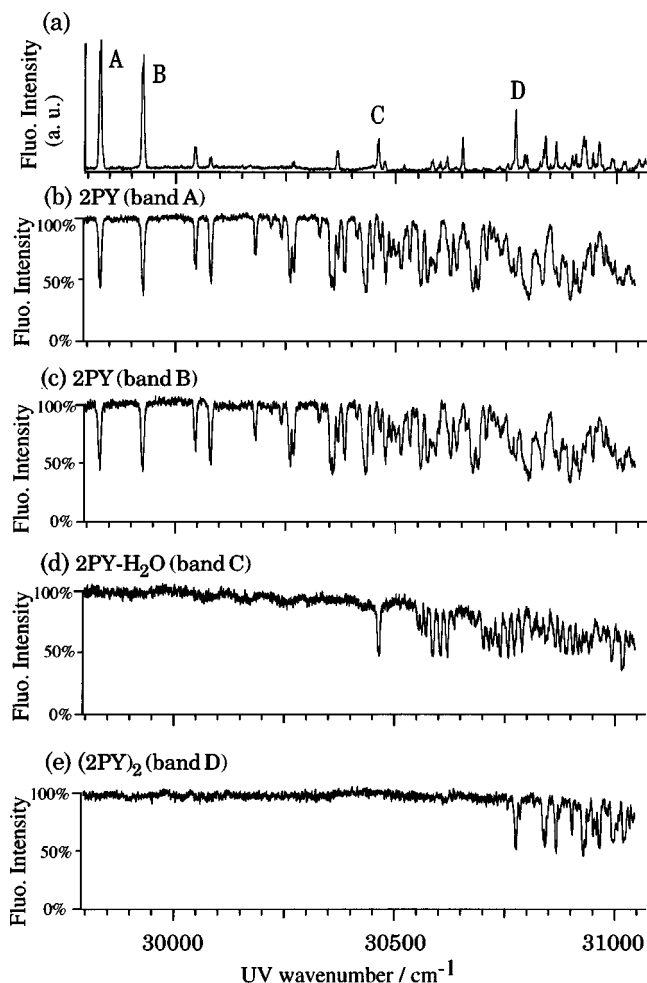


FIG. 4. (a) LIF spectra of 2PY and its hydrogen-bonded cluster. (b), (c) Population labeling spectra obtained by fixing the probe laser frequencies to bands A and B of the 2PY monomer. (d) Population labeling spectra of 2PY-H<sub>2</sub>O obtained by monitoring band C. (e) Population labeling spectrum of (2PY)<sub>2</sub> obtained by monitoring band D. Pump and probe laser powers were set at  $\sim 200$  and  $5 \mu\text{J}$ , respectively.

ing the conclusion that they belong to the same isomer of 2PY.

We then measured population-labeling spectra to obtain further evidence of the single isomer of 2PY in  $S_0$ . Figure 4(a) shows the LIF spectrum of 2PY in a wider energy region, and Figs. 4(b) and 4(c) show the population labeling spectra of 2PY obtained by tuning the probe laser frequency to the bands A and B, respectively. As seen in Fig. 4, the two spectra show essentially an identical vibronic structure. From this result and from the fact that band A is assigned to the  $S_1$  band origin, it is concluded that the band B also originated from the zero-point level of  $S_0$  of the same species.

As seen in Fig. 4(a), there are not so many bands in the higher energy region of the LIF spectrum, while in Figs. 4(b) and 4(c) many intense bands appear in the higher energy region of the population labeling spectra. The results indicate a rapid decrease of the fluorescence quantum yield with the excitation energy. By comparing the relative band intensities between the LIF and the population labeling spectra, relative fluorescence quantum yields of the vibronic bands can be obtained. The population-labeling spectrum can be converted

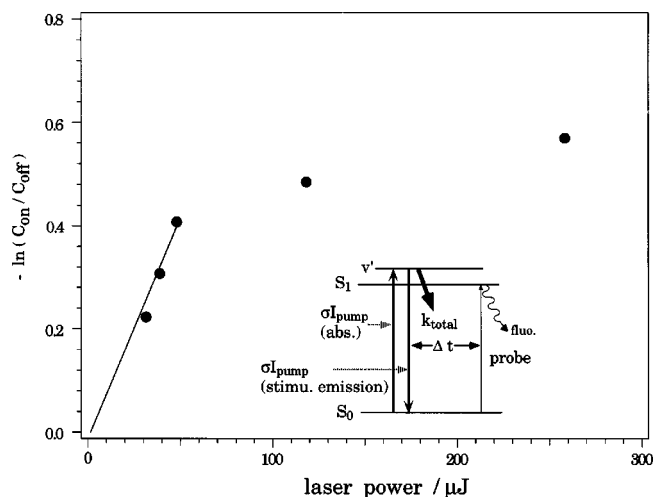


FIG. 5. (a) Plot of  $-\ln(C_{\text{on}}/C_{\text{off}})$  vs the pump laser power for band A and the excitation scheme. See the text.

to the absorption spectrum by using a rate equation model based on the excitation scheme given in Fig. 5. The electronic transition cross section can be expressed by the following equation under a weak  $\nu_{\text{pump}}$  power condition, so that the  $S_1$ - $S_0$  transition is not saturated:<sup>48</sup>

$$\sigma I_{\text{pump}} \Delta t \propto -\ln(C_{\text{on}}/C_{\text{off}}). \quad (1)$$

Here, we also assume that the rate of the reverse process, that is the stimulated emission pumping, is much smaller than the decay rate of  $S_1$ . This condition can also be satisfied under the weak laser power condition.<sup>54</sup> In Eq. (1),  $\sigma$  represents the  $S_1$ - $S_0$  absorption cross section and  $I_{\text{pump}}$  is the  $\nu_{\text{pump}}$  laser power and  $\Delta t$  is its pulse width.  $C_{\text{on}}$  and  $C_{\text{off}}$  are the ground state populations when  $\nu_{\text{pump}}$  is resonant and off-resonant with the electronic transition, respectively. The relative values,  $C_{\text{on}}$  and  $C_{\text{off}}$ , are obtained as intensities of laser-induced fluorescence by the probe laser ( $\nu_{\text{probe}}$ ). This laser power is set very weak (typically  $5 \mu\text{J}$ ) so that it does not affect the ground state population. Figure 5 shows a plot of  $-\ln(C_{\text{on}}/C_{\text{off}})$  versus the  $\nu_{\text{pump}}$  power for band A. As shown in Fig. 5, a linear relationship is seen for the  $\nu_{\text{pump}}$  power below  $50 \mu\text{J}$ . Thus, we measured the population-labeling spectrum under the  $\nu_{\text{pump}}$  power below  $50 \mu\text{J}$ , and transformed it to the absorption spectrum by using Eq. (1). The resulting absorption spectrum shown in Fig. 6(a) is compared with the LIF spectrum of Fig. 6(b), and the relative fluorescence quantum yields are plotted in Fig. 6(c). There are several noticeable points in the obtained fluorescence quantum yields of the vibronic bands. First, more than 20 vibronic bands appear within the  $1000 \text{ cm}^{-1}$  region above the 0,0 band. Second, as was mentioned previously, the fluorescence quantum yield rapidly decreases with the energy. Finally, there are several bands whose relative fluorescence quantum yield is anomalously weak even at the lower energy region. These bands are marked by open triangles in the energy region up to  $700 \text{ cm}^{-1}$  above the band origin. Actually these bands are completely missing in the LIF spectrum.

The rapid decrease of the fluorescence quantum yield with the excitation energy may be interpreted by the increase of nonradiative decay rates, such as internal conversion or



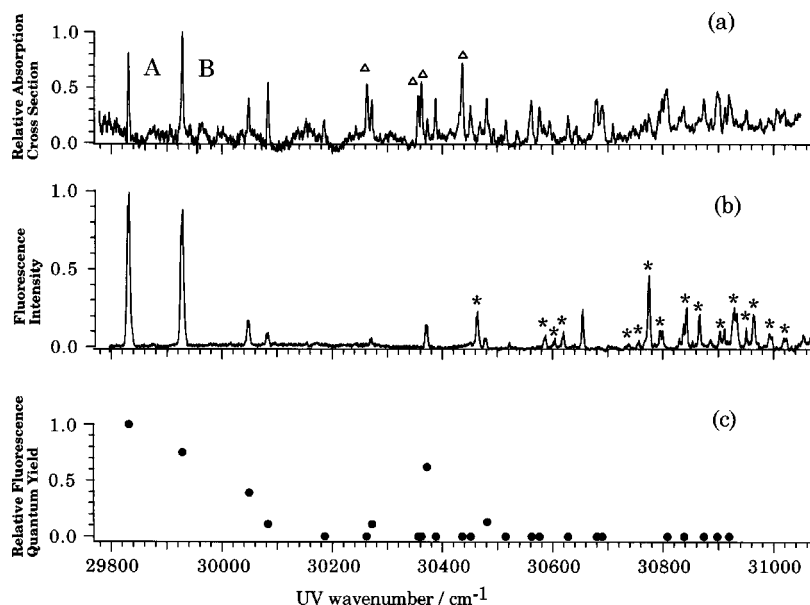


FIG. 6. (a) Transformed population labeling spectrum of 2PY by using Eq. (1). The bands marked by open triangles are the bands which are missing in the LIF spectrum. (b) LIF spectrum of 2PY. The bands marked by asterisks are the vibronic bands of clusters. (c) Plots of the relative fluorescence quantum yields of the vibronic bands vs the energy, which is normalized to that of band A.

intersystem crossing. On the other hand, the bands which are completely missing in the LIF spectrum even at the lower energy region may be described either by a strong mode dependence of their nonradiative decay rates or by the appearance of the vibronic bands of the electronic state lower than the  $S_1(\pi\pi^*)$  state, such as the  $n\pi^*$  state. As to the latter case, the  $n\pi^*$  state is observed below  $S_1(\pi\pi^*)$  in the 2PH form. In contrast, there has been no report for the state for 2PY form.<sup>5,17,29</sup> Thus, there is little possibility of the presence of the  $n\pi^*$  state below  $S_1$ . However, as seen in Fig. 6(a), the population labeling spectra shows a very complicated vibronic structure, suggesting a perturbation by other states. So, the two possibilities raised above cannot be distinguished at this moment.

## 2. 2PY-H<sub>2</sub>O

The population labeling spectrum of 2PY-H<sub>2</sub>O observed by fixing the probe laser to band C at 30 465 cm<sup>-1</sup> is shown in Fig. 4(d), and the absorption spectrum transformed by using Eq. (1) is shown in Fig. 7(a). The spectrum is very similar to the mass resolved resonance enhanced multiphoton ionization spectrum of 2PY-H<sub>2</sub>O measured by Nimlos, Kelley, and Bernstein<sup>38</sup> and no band is observed below the band at 30 465 cm<sup>-1</sup>, leading to the conclusion that this band is the  $S_1-S_0$  origin. The spectrum shows very rich vibrational structure and no prominent band corresponding to band B of the 2PY monomer is seen at 100 cm<sup>-1</sup> above the band origin. Instead, in the energy region of 140 cm<sup>-1</sup>, there are three equal intensity bands with their spacing of 17 cm<sup>-1</sup>. One of them is assigned to the intermolecular stretching vibration in  $S_1$ , since the frequencies are similar to those of the other hydrogen-bonded clusters, such as phenol-H<sub>2</sub>O<sup>55</sup> or naphthol-H<sub>2</sub>O.<sup>56</sup> Actually, a progression of  $\sim 180$  cm<sup>-1</sup> is seen in the dispersed fluorescence spectrum of 2PY-H<sub>2</sub>O reported by Nimlos, Kelley, and Bernstein (Fig. 7 of Ref. 38), which may correspond to the intermolecular stretching vibration in  $S_0$ . Other bands in the 140 cm<sup>-1</sup> region may involve the transitions of the other excited states correspond-

ing to band B of bare 2PY. In the higher energy region, many bands are closely overlapped and they may be assigned to the combination bands of the intramolecular and intermolecular modes. Figure 7(c) shows a plot of the relative fluorescence quantum yield versus the excitation energy. Similar to 2PY monomer, the relative fluorescence quantum yield

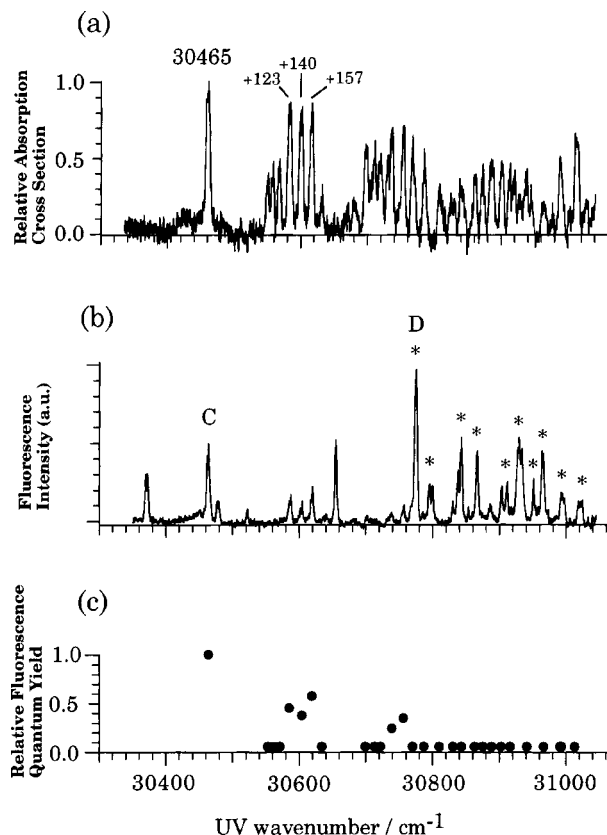


FIG. 7. (a) Transformed population labeling spectrum of 2PY-H<sub>2</sub>O. (b) LIF spectrum of 2PY, 2PY-H<sub>2</sub>O, and (2PY)<sub>2</sub>. The bands marked by asterisks are the bands belonging to (2PY)<sub>2</sub>. (c) Plots of the fluorescence quantum yields of the vibronic bands vs the energy, which is normalized to that of band origin.

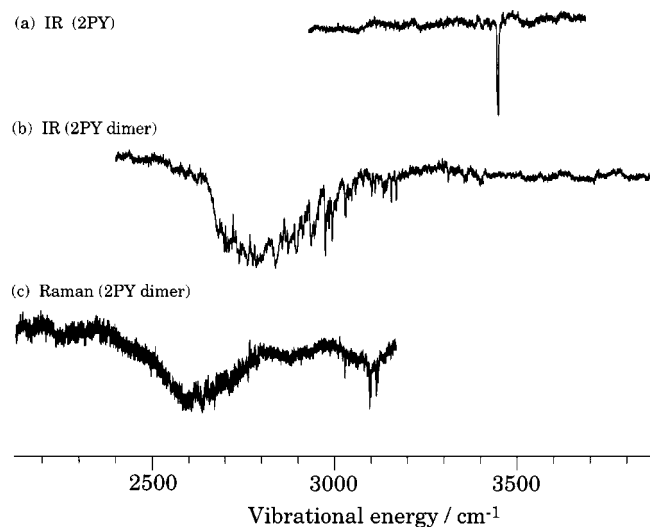


FIG. 8. FDIR spectra of (a) 2PY, (b)  $(2PY)_2$ , and (c) FDSR spectrum of  $(2PY)_2$  in the region of the NH stretching vibration in the  $S_0$  state.

decreases rapidly with the energy. Different from the monomer, however, it was difficult to identify missing bands in the low energy region for  $2PY-H_2O$ , because of the overlap of the monomer bands in the LIF spectrum.

### 3. $(2PY)_2$

Figure 4(e) shows the population-labeling spectrum of  $(2PY)_2$ , which was obtained by monitoring band *D* at  $30\,775\text{ cm}^{-1}$ . This band was first assigned to a vibronic band of 2PY dimer by Pratt and co-workers.<sup>40,43</sup> Since no band is observed below the band *D*, this band is assigned to the  $S_2(^1B_u)$  band origin of  $(2PY)_2$ . In our previous paper, we reported the IR spectrum of the NH stretching vibration of  $(2PY)_2$ . The observed IR active NH stretch vibration, which is assigned to the ungerade mode, was largely redshifted and very broad. In the present work, we measured the Raman spectrum to observe the band due to the gerade mode and also to confirm an intensity alternation between the IR and Raman spectra.

In Fig. 8, the FDSR spectrum of  $(2PY)_2$  is shown, being compared with the previously reported FDIR spectra. In the Raman spectrum of  $(2PY)_2$ , the broad NH stretching band is observed at  $2600\text{ cm}^{-1}$ , while the NH band in the IR spectrum occurs at  $2800\text{ cm}^{-1}$ . Such a clear difference between the IR and Raman spectra also represents the presence of the inversion symmetry in the dimer, and the bands at  $2600$  and  $2800\text{ cm}^{-1}$  are assigned to the gerade and ungerade modes of the NH stretching vibration, respectively. The result supports well the  $C_{2h}$  symmetry of  $(2PY)_2$ .<sup>28,40,44</sup> The large redshifts of the NH stretch vibrations in the dimer,  $850\text{ cm}^{-1}$  for gerade mode and  $650\text{ cm}^{-1}$  for ungerade mode, are due to large binding energy of the hydrogen bond in  $(2PY)_2$ . The binding energy of  $(2PY)_2$  was experimentally obtained to be  $14.8\text{ kcal/mol}$  by Fujimoto and Inuzuka<sup>28</sup> and very recently Müller, Talbot, and Leutwyler, reported the energy to be  $17.23\text{ kcal/mol}$  by density functional calculation.<sup>44</sup>

Another noticeable point of the NH stretching bands of  $(2PY)_2$  is its anomalously broad feature. The widths (full

width at half-maximum) of the NH bands in the FDSR and FDIR spectra are  $150$  and  $250\text{ cm}^{-1}$ , respectively. Since the bands in the spectra are attributed to the transitions from the zero-point level of  $(2PY)_2$ , no hot band is involved in the spectra. Thus the broadness of the NH bands are attributed partly to the appearance of many other vibrations and also to the broadening by strong anharmonic couplings with the NH stretching vibration which leads to the fast intracluster vibrational redistribution. Among several vibrations, CH stretching vibrations are the possible candidates for the coupling with the NH stretching vibration. As was described in the previous paper,<sup>45</sup> the NH stretching vibration lies close to the CH stretching vibrations upon the hydrogen bond formation. In this case, the NH stretch vibration may couple with the CH stretch modes and the observed vibrational bands will be linear combinations of the NH and the CH modes. Actually, sharp CH vibration, which are very weak in bare 2PY, appeared strongly at the higher frequency side of the NH band in the IR spectrum. However, in the Raman spectrum of Fig. 8(a), the CH bands appear at  $3100\text{ cm}^{-1}$  and are completely separated from the NH band. Thus, the coupling with the overtone and/or combinations may be much more responsible for the broadening of the Raman spectrum.

## B. Vibrational spectra of 2PY and its clusters in $S_1$

### 1. 2PY

As described in a previous section, it is concluded that the bands *A* and *B* of 2PY belong to the same species in  $S_0$ . Then a question occurs whether band *B* is a vibronic band of band *A*. Most useful information for this question is the measurements of the dispersed fluorescence (DF) spectra by exciting the two bands. Actually, Nimlos, Kelley, and Bernstein<sup>38</sup> observed the DF spectra for the two bands and the two spectra were very similar to each other and no low frequency vibration was seen in either spectrum. Thus, this result suggests that the *B* band is not the vibronic band accompanying the *A* band, and the two bands should be assigned to the band origins of slightly different species in the excited electronic state.

To obtain more information for the structure of 2PY monomer in the excited electronic state, we measured the IR spectrum of the NH stretching vibration of the excited state by UV-IR double-resonance spectroscopy. Figure 9(a) shows the UV-IR double-resonance spectra of bands *A* and *B* in the NH and CH stretching vibrational region. In both spectra, the NH stretching band in the excited state appears at  $\sim 3410\text{ cm}^{-1}$ , which is smaller by  $38\text{ cm}^{-1}$  than that in  $S_0$ . In the two spectra there is a small but clear difference in their NH vibrational frequencies. In the lower part of Fig. 9 are shown the enlarged spectra of the (b) CH and the (c) NH stretching bands. As seen in the figure, the CH stretching bands appear at the same frequencies, while the frequencies of the NH stretching bands differ by  $1.8\text{ cm}^{-1}$  between the spectra of bands *A* and *B*. The difference is additional evidence of the different structures of the upper states for the bands *A* and *B* reported by Held and Pratt.<sup>43</sup> It is not clear whether they belong to the different electronic states, such as  $S_1$  and  $S_2$ , or the isomers in the same electronic state. From

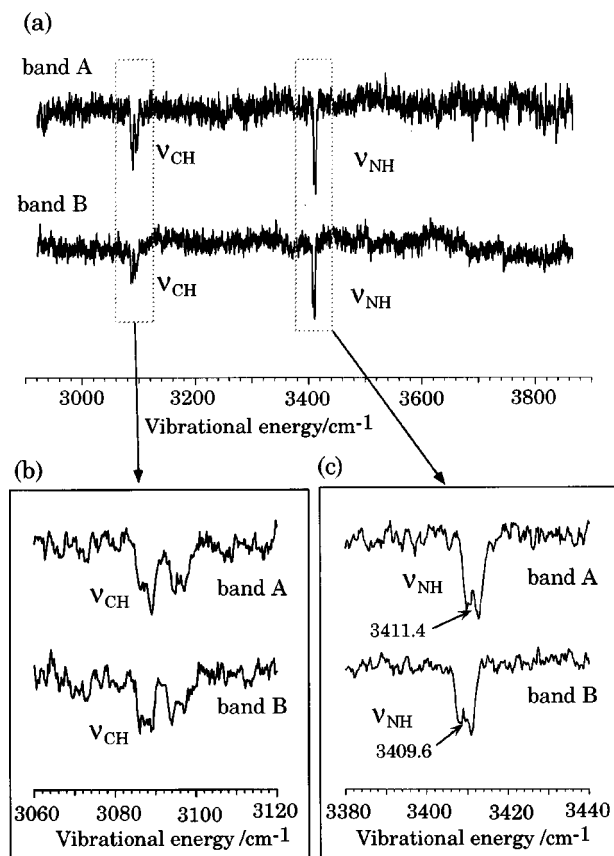


FIG. 9. (a) UV-IR double-resonance spectra of bands A and B of 2PY monomer in the  $S_1$  state. (b) Enlarged portion of the CH stretching region. (c) Enlarged portion of the NH stretching vibrational region.

the similarity of the dispersed fluorescence spectra, the structural difference is very small, so we hereafter refer to both excited states as  $S_1$ .

## 2. 2PY-H<sub>2</sub>O and (PY)<sub>2</sub>

As shown previously, the NH stretching frequency of the 2PY monomer in  $S_1$  is  $38\text{ cm}^{-1}$  lower than that in  $S_0$ , suggesting that the electronic excitation may also change the hydrogen bonding capability of 2PY. The change of the hydrogen bonding strength can be observed by the redshift of the NH and also of the OH stretching vibrations of the hydrogen bonded cluster. So, we measured the IR spectrum of 2PY-H<sub>2</sub>O in  $S_1$ , which is shown in Fig. 10(b). The spectrum is compared with that of bare 2PY [Fig. 10(a)]. As seen in the figures, the hydrogen-bonded NH and OH stretching vibrations are widely separated. The frequency reduction of the NH stretch of 2PY-H<sub>2</sub>O from that of bare 2PY in  $S_1$  is  $123\text{ cm}^{-1}$ . The corresponding vibrational spectrum of 2PY-H<sub>2</sub>O in  $S_0$  was reported in our previous paper.<sup>45</sup> In  $S_0$ , hydrogen-bonded NH and OH stretching vibrations lie close to each other at  $3340\text{ cm}^{-1}$  and the frequency reduction of the NH stretch of 2PY-H<sub>2</sub>O from that of bare 2PY is  $119\text{ cm}^{-1}$ . Thus, the NH-O hydrogen bond strength is not so different between the two electronic states. On the other hand, the reductions of the OH stretch frequencies in  $S_0$  and  $S_1$  are found to be  $211$  and  $72\text{ cm}^{-1}$ , respectively. So, the reduction of the OH stretching frequency of the H<sub>2</sub>O site

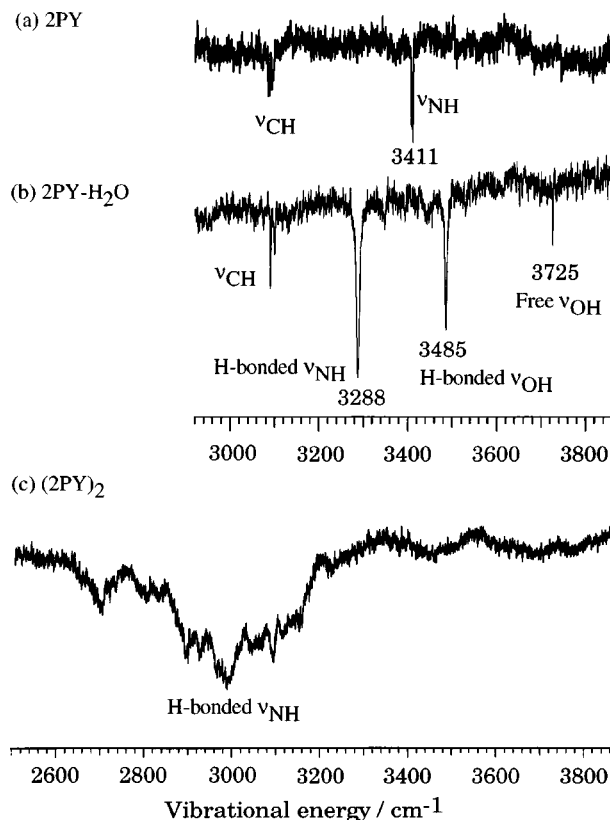


FIG. 10. UV-IR double-resonance spectra of (a) 2PY, (b) 2PY-H<sub>2</sub>O, and (c) (2PY)<sub>2</sub> in the  $S_1$  state.

upon the hydrogen bond formation in  $S_1$  is smaller than in  $S_0$ . From these results, it is concluded that the hydrogen bond strength between H<sub>2</sub>O and the C=O group of 2PY in  $S_1$  is weaker than in  $S_0$ , while that between H<sub>2</sub>O and the NH group is almost the same. Pratt and co-workers reported that the intermolecular distance of 2PY-H<sub>2</sub>O increases in  $S_1$ .<sup>42</sup> Thus, all these results show that the hydrogen bond strength between the C=O group of 2PY and the OH group of H<sub>2</sub>O become weaker in  $S_1$ . It also explains the observed blueshift of the  $S_1$ - $S_0$  electronic transition 2PY-H<sub>2</sub>O.

A similar decrease of the hydrogen bond strength was observed in  $S_1$  of (2PY)<sub>2</sub>. Figure 10(c) shows the IR spectrum of the NH stretch vibration of (2PY)<sub>2</sub> in  $S_1$ . The observed band has a peak at  $\sim 3000\text{ cm}^{-1}$  and its redshift from that of the monomer is  $410\text{ cm}^{-1}$ . This redshift is substantially smaller than that ( $650\text{ cm}^{-1}$ ) in  $S_0$ , indicating that the hydrogen bond strength of (2PY)<sub>2</sub> is also weakened in  $S_1$ . This result also agrees with the result obtained from the high resolution LIF spectrum by Held and Pratt.<sup>43</sup> Actually, Weisstuch, Neidig, and Testa suggested that the acidity of 2PY decreases in  $S_1$  from the blueshift of anion emission relative to the neutral molecule.<sup>5</sup> Thus, it is interesting to note that 2PY shows a contradicting feature, that is, the NH bond strength is weakened while the acidity decreases upon the electronic excitation.

## IV. CONCLUSION

In the present work, we investigated the structures and electronic properties of 2PY and its hydrogen-bonded clus-



ters by using various spectroscopic methods. For 2PY monomer, bands *A* and *B*, which are lying close each other in the  $S_1$  band origin, were assigned to the origins of the different upper states whose structures involving the NH group are slightly different. It was found that the fluorescence quantum yield rapidly decreases with the energy and that several vibronic bands are nonfluorescent even in the low energy region. The NH stretching vibrations were observed for  $S_0$  and  $S_1$  and it was found that the NH stretching frequency is reduced by  $38\text{ cm}^{-1}$  upon the excitation to  $S_1$ . Thus, the NH bond strength is slightly weakened in  $S_1$ . As to the tautomerization of 2PY in  $S_1$ , Nowak *et al.* observed transformation of 2PY to 2PH by the UV irradiation of matrix isolated 2PY/2PH. They suggested the ring opening reaction for this transformation because they observed of the vibration which may be assigned to the antisymmetric vibration of  $=C=O$  group. The observed weakening of the NH bond strength in  $S_1$  in the present work may be related to the ring open reaction or may promote intramolecular proton transfer in the intermediate state.

On the other hand, it was found that the hydrogen-bond strengths of 2PY– $H_2O$  and  $(2PY)_2$  are weakened in  $S_1$  due to a decrease of the acidity of 2PY. The decrease of hydrogen bond strength in  $S_1$  decelerates the tautomerization reaction of 2PY in protic solvent molecules. This is because that the reaction in protic solvents is thought to occur through the proton exchange in the ring-form intermediates, such as shown in Figs. 1(b) and 1(c), and the decrease of the hydrogen bond, that is the increases the  $OH-O=C$  distance, will act to inhibit the reaction. Thus, it is not clear whether the tautomerization reaction is promoted or prohibited in the clusters involving the 2PY form in  $S_1$  and it will be very interesting to perform similar experiments for the clusters involving 2HP form.

## ACKNOWLEDGMENTS

The authors wish to thank Dr. A. Fujii, Dr. H. Ishikawa, and Dr. T. Maeyama for their helpful discussions. This work is supported in part by the Grant-in-Aids for Scientific Research (No. 10440165) by the Ministry of Education, Science sports and Culture, Japan.

- <sup>1</sup>S. F. Mason, J. Chem. Soc. 674 (1958).
- <sup>2</sup>B. Pullman and A. Pullman, Adv. Heterocycl. Chem. **13**, 77 (1971).
- <sup>3</sup>M. J. Cook, A. R. Katritzky, P. Linda, and R. D. Tack, J. Chem. Soc., Perkin Trans. 2 **2**, 1295 (1972).
- <sup>4</sup>P. Beak and F. S. Fry, Jr., J. Am. Chem. Soc. **95**, 1700 (1973).
- <sup>5</sup>A. Weisstuch, P. Neidig, and A. C. Testa, J. Lumin. **10**, 137 (1975).
- <sup>6</sup>P. Beak, F. S. Fry, Jr., J. Lee, and F. Steele, J. Am. Chem. Soc. **98**, 171 (1976).
- <sup>7</sup>M. J. Cook and A. R. Katritzky, Tetrahedron Lett. **31**, 2685 (1976).
- <sup>8</sup>P. Beak, Acc. Chem. Res. **10**, 186 (1977).
- <sup>9</sup>O. Bensaude, M. Dreyfus, G. Dodin, and J. E. Dubois, J. Am. Chem. Soc. **99**, 4438 (1977).
- <sup>10</sup>O. Bensaude, M. Chevrier, and J.-E. Dubois, J. Am. Chem. Soc. **101**, 2423 (1979).
- <sup>11</sup>C. Guimon, G. Garrabe, and G. Pfister-Guillouzo, Tetrahedron Lett. 2585 (1979).
- <sup>12</sup>R. S. Brown, A. Tse, and J. C. Vederas, J. Am. Chem. Soc. **102**, 1174 (1980).
- <sup>13</sup>J. S. Kwiatkowski and B. Szczodrowska, Chem. Phys. **27**, 389 (1978).
- <sup>14</sup>J. S. Kwiatkowski and A. Tempczyk, Chem. Phys. **85**, 397 (1981).
- <sup>15</sup>C. Krebs, H. J. Hofmann, H. J. Kohler, and C. Weiss, Chem. Phys. Lett. **69**, 537 (1980).
- <sup>16</sup>A. Lledos and J. Bertran, Tetrahedron Lett. **22**, 775 (1981).
- <sup>17</sup>A. Fujimoto, K. Inuzuka, and R. Shiba, Bull. Chem. Soc. Jpn. **54**, 2802 (1981).
- <sup>18</sup>H.-J. Hofmann, G. Peinel, C. Krebs, and C. Weiss, Int. J. Quantum Chem. **20**, 785 (1981).
- <sup>19</sup>J. S. Kwiatkowski and A. Tempczyk, Chem. Phys. **85**, 397 (1981).
- <sup>20</sup>C. Krebs, W. Forster, C. Weiss, and H. J. Hofmann, J. Prakt. Chem. **324**, 369 (1982).
- <sup>21</sup>H. B. Schlegel, P. Gund, and E. M. Fluder, J. Am. Chem. Soc. **104**, 5347 (1982).
- <sup>22</sup>M. J. Scanlan, I. H. Hillier, and A. A. MacDowell, J. Am. Chem. Soc. **105**, 3568 (1982).
- <sup>23</sup>M. J. Scanlan and I. H. Hillier, Chem. Phys. Lett. **107**, 330 (1984).
- <sup>24</sup>R. S. Brown, A. Tse, and J. C. Vederas, J. Chem. Soc. Chem. Commun. 435 (1984).
- <sup>25</sup>M. J. Field, I. H. Hillier, and M. F. Guest, J. Chem. Soc. Chem. Commun. 1310 (1984).
- <sup>26</sup>M. J. Scanlan and I. H. Hillier, Chem. Phys. Lett. **107**, 330 (1984).
- <sup>27</sup>M. Kuzuya, A. Noguchi, and T. Okuda, J. Chem. Soc. Chem. Commun. 435 (1984).
- <sup>28</sup>A. Fujimoto and K. Inuzuka, Spectrochim. Acta A **41**, 1471 (1985).
- <sup>29</sup>R. Tembreull, C. H. Sin, H. M. Pang, and D. M. Lubman, Anal. Chem. **57**, 2911 (1985).
- <sup>30</sup>A. Lledos and J. Bertran, J. Mol. Struct.: THEOCHEM **120**, 73 (1985).
- <sup>31</sup>P. Cieplak, P. Bash, U. C. Singh, and P. A. Kollman, J. Am. Chem. Soc. **109**, 6283 (1987).
- <sup>32</sup>M. J. Nowak, L. Lapinski, J. Fulara, A. Les, and L. Adamowicz, J. Phys. Chem. **96**, 1562 (1992).
- <sup>33</sup>L. D. Hatherley, R. D. Brown, P. D. Godfrey, A. P. Pierlot, W. Caminati, D. Damiani, S. Merland, and L. B. Favero, J. Phys. Chem. **97**, 46 (1993).
- <sup>34</sup>A. L. Sobolewski and L. Adamowicz, J. Phys. Chem. **100**, 3933 (1996).
- <sup>35</sup>J. Wang and R. J. Boyd, J. Phys. Chem. **100**, 16141 (1996).
- <sup>36</sup>P. T. Chou, C. Y. Wei, and F. T. Hung, J. Phys. Chem. B **101**, 9119 (1997).
- <sup>37</sup>A. Dkhissi, L. Houben, J. Smets, L. Adamowicz, and G. Maes, J. Mol. Struct. **484**, 215 (1999).
- <sup>38</sup>M. R. Nimlos, D. F. Kelley, and E. R. Bernstein, J. Phys. Chem. **93**, 643 (1989).
- <sup>39</sup>A. Held, B. B. Champagne, and D. W. Pratt, J. Chem. Phys. **95**, 8732 (1989).
- <sup>40</sup>A. Held and D. W. Pratt, J. Am. Chem. Soc. **112**, 8629 (1990).
- <sup>41</sup>A. Held and D. W. Pratt, J. Am. Chem. Soc. **115**, 9708 (1993).
- <sup>42</sup>A. Held and D. W. Pratt, J. Am. Chem. Soc. **115**, 9718 (1993).
- <sup>43</sup>A. Held and D. W. Pratt, J. Chem. Phys. **96**, 4869 (1992).
- <sup>44</sup>A. Müller, F. Talbot, and S. Leutwyler, J. Chem. Phys. **112**, 3717 (2000).
- <sup>45</sup>Y. Matsuda, T. Ebata, and N. Mikami, J. Chem. Phys. **110**, 8397 (1999).
- <sup>46</sup>T. Ebata, *Population Labelling Spectroscopy*, Nonlinear Spectroscopy for Molecular Structure Determination, Vol. 6, edited by R. W. Field, E. Hirota, J. P. Maier, and S. Tsuchiya (Blackwell Science), pp. 149–165.
- <sup>47</sup>S. Tanabe, T. Ebata, and N. Mikami, Chem. Phys. Lett. **215**, 347 (1993).
- <sup>48</sup>T. Ebata, T. Watanabe, and N. Mikami, J. Phys. Chem. **99**, 5763 (1995).
- <sup>49</sup>S. Ishikawa, T. Ebata, and N. Mikami, J. Chem. Phys. **110**, 9504 (1999).
- <sup>50</sup>R. Yamamoto, S. Ishikawa, T. Ebata, and N. Mikami, Int. J. Raman Spectrosc. (in press).
- <sup>51</sup>N. Guichhait, T. Ebata, and N. Mikami, J. Am. Chem. Soc. **121**, 5705 (1999).
- <sup>52</sup>N. Guichhait, T. Ebata, and N. Mikami, J. Chem. Phys. **111**, 8438 (1999).
- <sup>53</sup>T. Ebata, N. Mizuochi, T. Watanabe, and N. Mikami, J. Phys. Chem. **100**, 546 (1996).
- <sup>54</sup>T. Suzuki and M. Ito, J. Phys. Chem. **91**, 3537 (1987).
- <sup>55</sup>T. Ebata, M. Furukawa, T. Suzuki, and M. Ito, J. Opt. Soc. Am. B **7**, 1890 (1990).
- <sup>56</sup>M. Schüte, T. Bürgi, S. Leutwyler, and T. Fischer, J. Chem. Phys. **99**, 1469 (1993).